

Supporting Information
For
**Unprecedented Ditungsten (0) Quadruply Bonded Complex Supported by π -
Donor Ligands**

Karen Ventura, Jacob R. Prat, Luis. M. Aguirre Quintana, Alan Goos and Dino Villagrán*

Department of Chemistry, University of Texas at El Paso, El Paso, Texas 79668

Table of Contents

Materials and methods	1
Computational Details	2
Figure S1. Select molecular orbital plots for orbitals showing strong π interactions.	3
X-ray Crystal Structure of 2 , $W_2(DippF)_2Cl_4Li \cdot 4THF$	4
Table S1. Sample and crystal data for 2 , $(W_2(DippF)_2Cl_4Li)$	5
Table S2. Data collection and structure refinement for 2 , $(W_2(DippF)_2Cl_4Li)$	6
X-ray Crystal Structure of 3 , $W_2(DippF)_2K_2$	7
Table S3. Sample and crystal data for 3 , $(W_2(DippF)_2K_2)$	8
Table S4. Data collection and structure refinement for 3 , $(W_2(DippF)_2K_2)$	9
Table S5. Calculated and experimental data for compound 3	10
Figure S2. EPR spectrum of compound 2 showing an isotropic signal with a g value of 1.86	11
Figure S3. Raman Spectrum for 3 ($W_2(DippF)_2K_2$). The $\nu(W-W)$ can be observed at 299.4 cm^{-1} . Strong ligand vibrations were observed at 343.7 and 421.8 cm^{-1}	12
Figure S4. ORTEP diagram of 2 plotted at the 50% probability value. W(1)-W(1) distance $2.280(1)\text{ \AA}$, W1-N(1) distance $2.130(1)\text{ \AA}$	13
Figure S5. NMR spectrum of compound 1 in d-THF.	14
Figure S6. NMR spectrum of compound 3 in d-THF.	15
Figure S7. UV-vis spectrum of compound 3	16
References:	17

Materials and methods

General. Standard vacuum line, dry-box, and Schlenk techniques under nitrogen atmosphere were employed for the synthesis of all compounds. All solvents were dried and degassed using a Pure Process Technology solvent purification system prior to use. Tungsten tetrachloride and HDippF were synthesized according to previously reported literature procedures.^{1,2}

Physical Measurements. ¹H NMR spectrum was recorded in a J Young NMR tube on a Bruker 400 MHz NMR spectrometer. The proton chemical shifts (δ) of **1** and **3** were referenced to the residual THF ($\delta = 1.72, 3.58$) in *d*-THF solvent. Raman Spectrum was recorded on a Thermo Scientific™ DXR SmartRaman spectrometer using a 780 cm⁻¹ filter. Electrochemical analysis was performed in THF using a CHI760D potentiostat with a 2 mm diameter Pt working electrode, Pt mesh auxiliary electrodes and Ag/Ag⁺ (AgCl) reference electrode. All potentials were subsequently internally referenced to the ferrocene/ferrocenium couple by adding ferrocene to the sample at the end of each run. The X-band (~ 9.5 GHz) EPR spectrum was obtained using a BrukerEMXplus spectrometer with an ER073 magnet at room temperature.

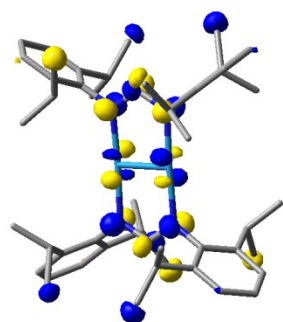
Preparation of W₂(DippF)₂Cl₄ (1). WCl₄ (0.500 g, 1.50 mmol) was reacted with KC₈ (0.417 g, 3.00 mmol) in 30 mL of THF at -94°C (liquid N₂ and acetone bath) under N₂ atmosphere until deep green coloration was observed. In a separate flask, LiDippF was prepared by reacting HDippF (0.557g, 1.50 mmol) and methyllithium (1.05mL, 1.68mmol) in 10 mL of THF at 0°C. The lithium formamidinate salt formed upon warming the solution to room temperature. It was then slowly added with a double tipped needle (cannula), for a period of 2 min, to the reduced ditungsten solution. The color turned dark blue after c.a. 1.5 h then the solution was filtered through a medium coarse filter packed with Celite®. The solvent was removed under reduced pressure, and the obtained red solid was washed thoroughly with diethyl ether and hexanes, and dried under vacuum. Isolated yield 0.830g, 25.85%. ¹H NMR spectroscopy (*d*-THF): δ 7.42 (s, 2H N-CH-N), 6.92-6.72 (m, 12H, *i*-Pr₂-C₆H₃), 3.62(septet, 8H, CHMe₂), 1.12 (d, 48H, (CH(CH₃)₂) (Figure S5). CV (V vs. Fc/Fc⁺): E'_{ap}: -1.271, E'_{cp}: -1.287, E'_{1/2}: -1.279, E''_{cp}: -1.898, E''_{ap}: -2.206, E''_{cp}: -2.720, E''_{1/2}: -2.46.

Preparation of W₂(DippF)₂Cl₄Li (2). 0.475g of compound **1** was reacted with 0.475g of Li metal in a Schlenk flask in THF. The solution was heated to reflux and left to react for ~ 1 hr. and filtered with a medium coarse filter. The solvent was removed under reduced pressure and extracted with hexanes. Yellow crystals were grown from a concentrated solution of THF. Isolated yield 0.471 g, 98.6%. EPR: g = 1.86.

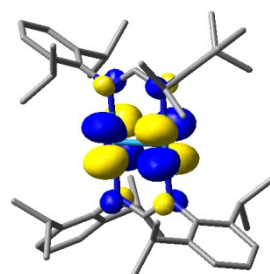
Preparation of W₂(DippF)₂K₂ (3). Compound **1** (0.200 g) was dissolved in 30 ml of THF. Potassium metal (1.00 g) was added to the resulting solution. The mixture was heated to reflux for two hours and then filtered through a medium coarse filter. The solvent was removed under reduced pressure and the product was extracted with diethyl ether. Amber- red crystals were grown from a concentrated solution of diethyl ether at -10°C. Isolated yield 0.027g, 13.58%. ¹H NMR spectroscopy (*d*-THF): δ 7.48 (s, 2H N-CH-N), 6.87-6.61 (m, 12H, *i*-Pr₂-C₆H₃), 3.62(septet, 8H, CHMe₂), 1.10 (d, 48H, (CH(CH₃)₂) (Figure S6). ESI-MS [M-CH₃]⁺: Calcd. 1157.4 found 1157.3 m/z.

Computational Details

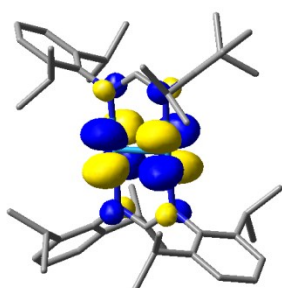
Density Functional Theory (DFT)^{3,4} calculations were performed with the hybrid Becke-3 parameter exchange functional⁵⁻⁷ and the Lee-Yang-Parr nonlocal correlation functional⁸ (B3LYP) implemented in the Gaussian 09⁹ (Revision C.01) program suit. Double- ζ -quality basis sets (D95) were used on nonmetal atoms (carbon, nitrogen and hydrogen). An effective core potential (ECP) representing the 1s2s2p3s3p3d core was used for the tungsten atoms along with the associated double- ζ basis set (LANL2DZ). The convergence criterion for the self-consistent field cycles on all calculations was increased from the default value to 10^{-8} . All the calculations were performed on a dianionic full-atom model of **3** with no simplifications. Geometry optimization calculations were found to be minima in the potential energy surface as evidenced by the lack of imaginary vibrations in the frequency calculations. Raman calculations were performed by using the keyword freq=raman in Gaussian. All calculations were performed in a 44-processor PowerWolf PSSC supercomputer cluster running Linux Red Hat 4.1.2-54 located at the University of Texas at El Paso.



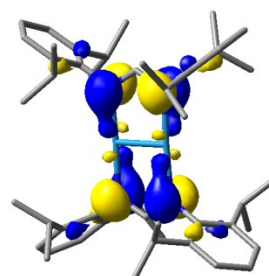
LUMO +16



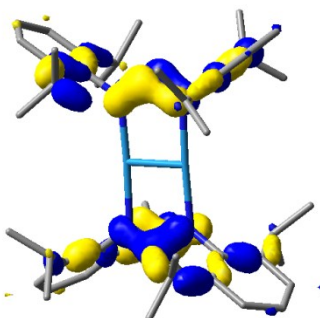
LUMO +14



LUMO +4



HOMO -7



HOMO -19

Figure S1. Select molecular orbital plots for orbitals showing strong π interactions.

X-ray Crystal Structure of 2, W₂(DippF)₂Cl₄Li•4THF

A yellow block specimen of C₅₀H₇₀Cl₄N₄W₂•C₁₆H₃₂LiO₄, approximate dimensions 0.100 mm x 0.100 mm x 0.050 mm, was used for the x-ray crystallographic analysis. The x-ray intensity data were measured.

The frames were integrated with the Bruker SAINT software package using a narrow-frame algorithm. The integration of the data using a monoclinic unit cell yielded a total of 71366 reflections to a maximum θ angle of 24.18° (1.00 Å resolution), of which 5451 were independent (completeness = 99.4%, $R_{\text{int}} = 11.40\%$, $R_{\text{sig}} = 10.15\%$) and 4689 (86.02%) were greater than $2\sigma(F^2)$. The final cell constants of $a = 23.7527(9)$ Å, $b = 12.0648(5)$ Å, $c = 25.981(1)$ Å, $\beta = 113.065(1)$ °, volume = 6850.2(5) Å³, are based upon the refinement of the XYZ-centroids of 4689 reflections above $2\sigma(I)$ with $3.72^\circ < 2\theta < 48.36^\circ$. Data were corrected for absorption effects using the multi-scan method (SADABS). The ratio of minimum to maximum apparent transmission was 0.788. The calculated minimum and maximum transmission coefficients (based on crystal size) are 0.5875 and 0.7453.

The structure was solved and refined using the Bruker SHELXTL Software Package, using the space group *C* 2/c, with $Z = 4$ for the formula unit, C₅₀H₇₀Cl₄N₄W₂•C₁₆H₃₂LiO₄. The final anisotropic full-matrix least-squares refinement on F^2 with 354 variables converged at $R1 = 10.15\%$, for the observed data and $wR2 = 21.53\%$ for all data. The goodness-of-fit was 1.226. The largest peak in the final difference electron density synthesis was 7.456 e⁻/Å³ and the largest hole was -3.690 e⁻/Å³ with an RMS deviation of 0.265 e⁻/Å³. On the basis of the final model, the calculated density was 1.485 g/cm³ and $F(000)$, 3108 e⁻.

Table S1. Sample and crystal data for **2**, (W₂(DippF)₂Cl₄Li).

Name	W ₂ (DippF) ₂ Cl ₄ Li	
Chemical formula	C ₅₀ H ₇₀ Cl ₄ N ₄ W ₂ •C ₁₆ H ₃₂ LiO ₄	
Formula weight	1531.94 g/mol	
Temperature	100(2) K	
Wavelength	0.71073 Å	
Crystal size	0.100 x 0.100 x 0.050 mm	
Crystal habit	clear yellow block	
Crystal system	monoclinic	
Space group	C 2/c	
Unit cell dimensions	a = 23.7527(9) Å	α = 90°
	b = 12.0648(5) Å	β = 113.065(1) °
	c = 25.981(1) Å	γ = 90°
Volume	6850.2(5) Å ³	
Z	4	
Density (calculated)	1.485 g/cm ³	
Absorption coefficient	3.559 mm ⁻¹	
F(000)	3108	

Table S2. Data collection and structure refinement for **2**, (W₂(DippF)₂Cl₄Li)

Theta range for data collection	1.86 to 24.18°
Index ranges	-27<=h<=27, -13<=k<=13, -29<=l<=29
Reflections collected	71366
Independent reflections	5451 [R(int) = 0.1140]
Coverage of independent reflections	99.4%
Absorption correction	multi-scan
Max. and min. transmission	0.7453 and 0.5875
Structure solution technique	direct methods
Structure solution program	SHELXT-2014/7 (Sheldrick, 2014)
Refinement method	Full-matrix least-squares on F ²
Refinement program	SHELXL-2014/7 (Sheldrick, 2014)
Function minimized	$\Sigma w(F_o^2 - F_c^2)^2$
Data / restraints / parameters	5451 / 361 / 354
Goodness-of-fit on F²	1.226
Δ/σ_{\max}	0.002
Final R indices	4689 data; I>2 σ (I) R1 = 0.1015, wR2 = 0.2071 all data R1 = 0.1170, wR2 = 0.2153
Weighting scheme	$w=1/[\sigma^2(F_o^2)+(0.0410P)^2+632.5916P]$ where $P=(F_o^2+2F_c^2)/3$
Largest diff. peak and hole	7.456 and -3.690 eÅ ⁻³
R.M.S. deviation from mean	0.265 eÅ ⁻³

X-ray Crystal Structure of 3, W₂(DippF)₂K₂

An amber- red plate-like specimen of C₁₁₆H₁₇₆K₄N₈O₄W₄, approximate dimensions 0.100 mm x 0.100 mm x 0.200 mm, was used for the X-ray crystallographic analysis. The X-ray intensity data were measured.

The total exposure time was 8.55 hours. The frames were integrated with the Bruker SAINT software package using a narrow-frame algorithm. The integration of the data using a triclinic unit cell yielded a total of 28893 reflections to a maximum θ angle of 20.84° (1.00 Å resolution), of which 6451 were independent (average redundancy 4.479, completeness = 96.6%, $R_{\text{int}} = 9.71\%$, $R_{\text{sig}} = 7.40\%$) and 4600 (71.31%) were greater than $2\sigma(F^2)$. The final cell constants of $a = 10.879(2)$ Å, $b = 13.364(3)$ Å, $c = 23.272(5)$ Å, $\alpha = 96.119(6)^\circ$, $\beta = 99.340(6)^\circ$, $\gamma = 105.700(6)^\circ$, volume = 3173.4(11) Å³, are based upon the refinement of the XYZ-centroids of 7004 reflections above $2\sigma(I)$ with $5.862^\circ < 2\theta < 41.61^\circ$. Data were corrected for absorption effects using the multi-scan method (SADABS). The ratio of minimum to maximum apparent transmission was 0.781. The calculated minimum and maximum transmission coefficients (based on crystal size) are 0.3140 and 0.5190.

The structure was solved and refined using the Bruker SHELXTL Software Package, using the space group P -1, with $Z = 1$ for the formula unit, C₁₁₆H₁₇₆K₄N₈O₄W₄. The final anisotropic full-matrix least-squares refinement on F^2 with 603 variables converged at $R1 = 7.40\%$, for the observed data and $wR2 = 24.46\%$ for all data. The goodness-of-fit was 1.113. The largest peak in the final difference electron density synthesis was 2.715 e⁻/Å³ and the largest hole was -2.428 e⁻/Å³ with an RMS deviation of 0.282 e⁻/Å³. On the basis of the final model, the calculated density was 1.377 g/cm³ and F(000), 1326 e⁻.

Table S3. Sample and crystal data for **3**, (W₂(DippF)₂K₂).

Name	W ₂ (DippF) ₂ K ₂	
Chemical formula	C ₁₁₆ H ₁₇₆ K ₄ N ₈ O ₄ W ₄	
Formula weight	2638.44 g/mol	
Temperature	100(2) K	
Wavelength	0.71073 Å	
Crystal size	0.100 x 0.100 x 0.200 mm	
Crystal habit	Amber red plate	
Crystal system	triclinic	
Space group	P -1	
Unit cell dimensions	a = 10.879(2) Å	α = 96.119(6)°
	b = 13.364(3) Å	β = 99.340(6)°
	c = 23.272(5) Å	γ = 105.700(6)°
Volume	3173.4(11) Å ³	
Z	1	
Density (calculated)	1.377 g/cm ³	
Absorption coefficient	3.791 mm ⁻¹	
F(000)	1326	

Table S4. Data collection and structure refinement for **3**, (W₂(DippF)₂K₂).

Theta range for data collection	2.39 to 20.84°
Index ranges	-10<=h<=10, -13<=k<=13, -23<=l<=23
Reflections collected	28893
Independent reflections	6451 [R(int) = 0.0971]
Coverage of independent reflections	96.6%
Absorption correction	multi-scan
Max. and min. transmission	0.5190 and 0.3140
Structure solution technique	direct methods
Structure solution program	SHELXT-2014/7 (Sheldrick, 2014)
Refinement method	Full-matrix least-squares on F ²
Refinement program	SHELXL-2014/7 (Sheldrick, 2014)
Function minimized	$\Sigma w(F_o^2 - F_c^2)^2$
Data / restraints / parameters	6451 / 661 / 603
Goodness-of-fit on F²	1.113
Δ/σ_{\max}	0.004
Final R indices	4600 data; I>2 σ (I) R1 = 0.0740, wR2 = 0.2002 all data R1 = 0.1165, wR2 = 0.2446
Weighting scheme	w=1/[$\sigma^2(F_o^2)+(0.1196P)^2+135.4914P$] where P=(F _o ² +2F _c ²)/3
Largest diff. peak and hole	2.715 and -2.428 eÅ ⁻³
R.M.S. deviation from mean	0.282 eÅ ⁻³

Table S5. Calculated and experimental data for compound **3**

Model	Atoms	Calculated Distance (Å)	Experimental Distance (Å)	Total Energy (Hartrees)	Experimental Raman (cm-1)	Calculated Raman (cm- 1)
3	W(1)-W(1A)	2.21	2.407(1)	-2302.17584346	299.4	313 (W-W)
	W(1)-N(1)	2.13	2.120(1)			
	W(1)-N(2A)	2.13	2.110(1)			

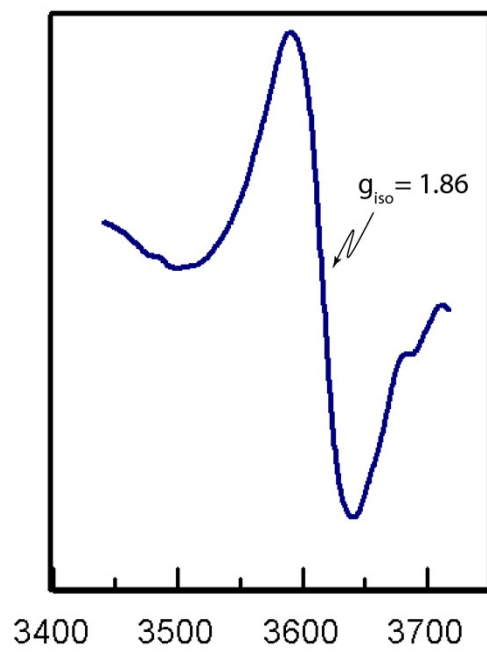


Figure S2. EPR spectrum of compound **2** showing an isotropic signal with a g value of 1.86

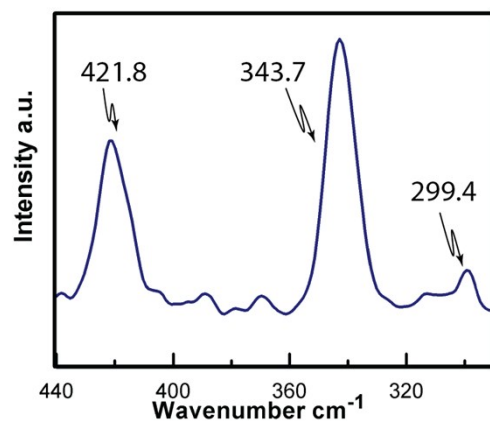


Figure S3. Raman Spectrum for **3** ($\text{W}_2(\text{DippF})_2\text{K}_2$). The $\nu(\text{W-W})$ can be observed at 299.4 cm^{-1} . Strong ligand vibrations were observed at 343.7 and 421.8 cm^{-1} .

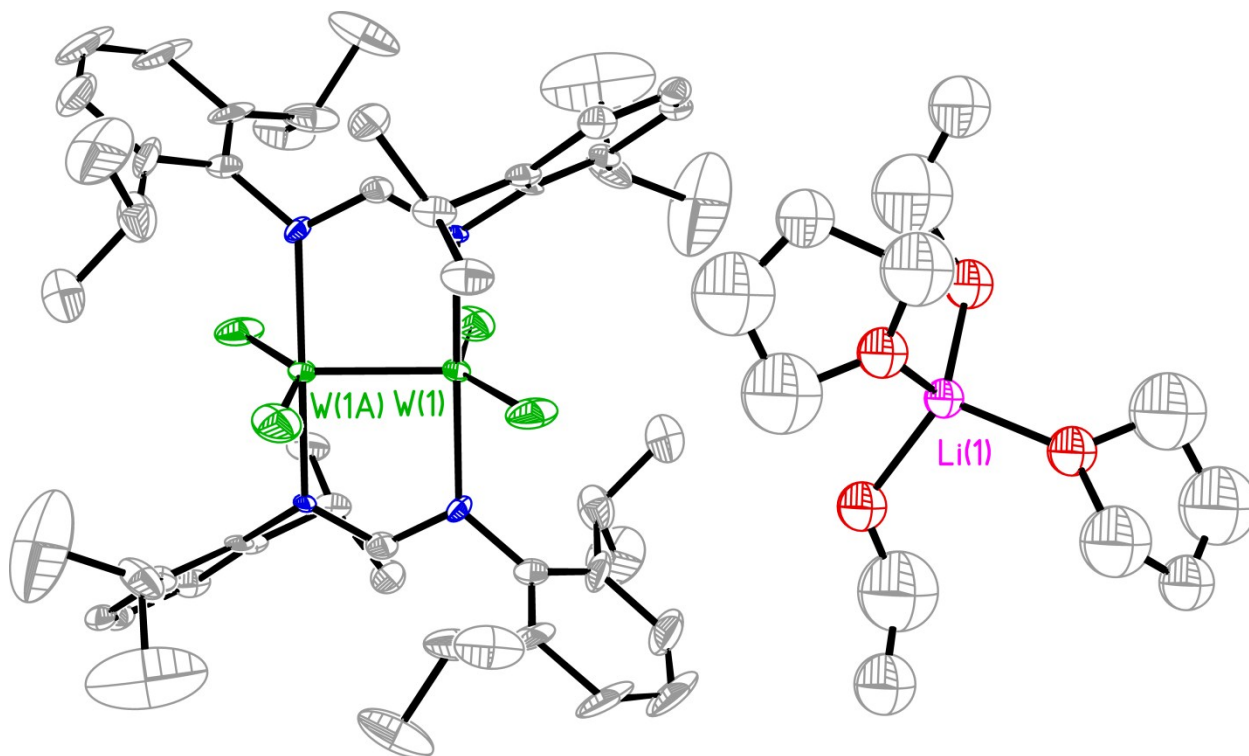


Figure S4. ORTEP diagram of **2** plotted at the 50% probability value. W(1)-W(1) distance 2.280(1) Å, W1-N(1) distance 2.130(1) Å.

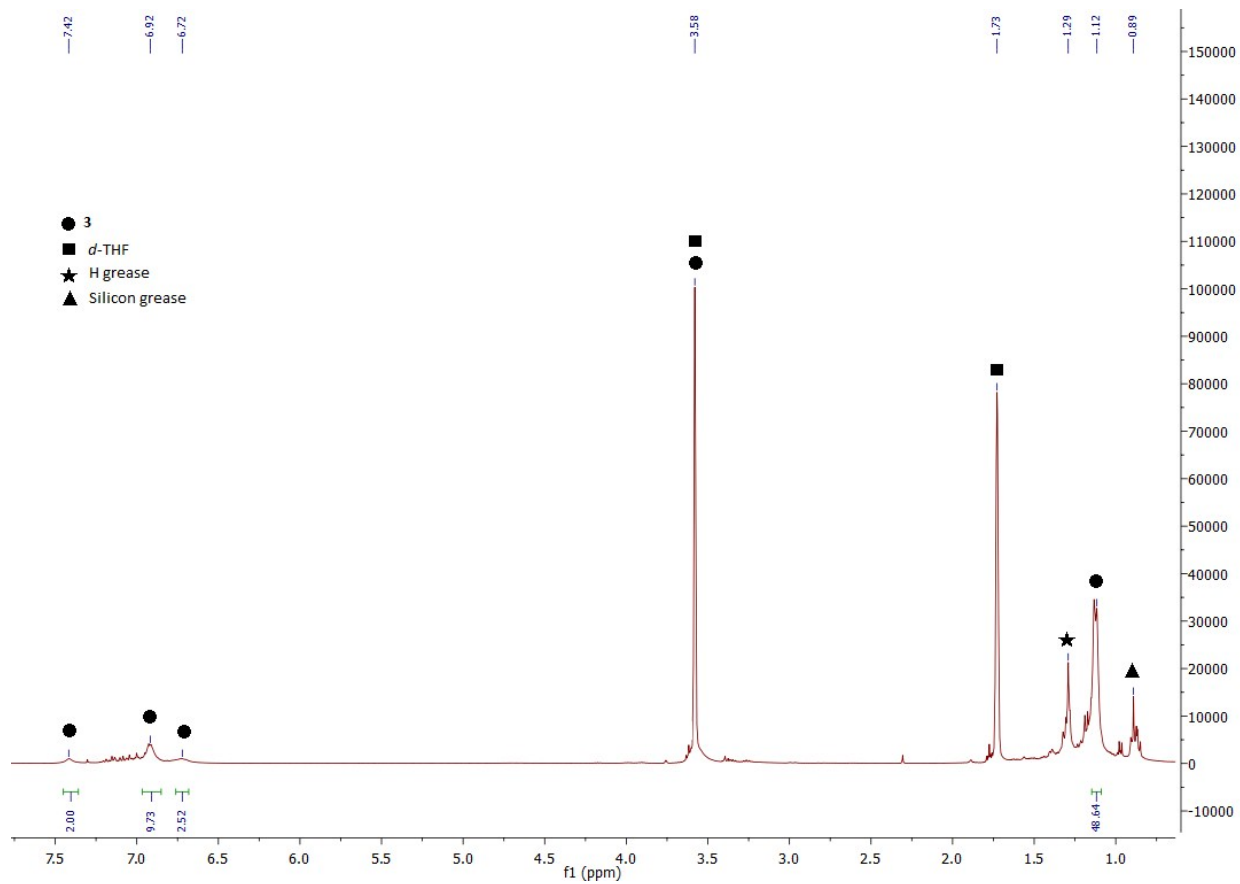


Figure S5. NMR spectrum of compound **1** in *d*-THF.

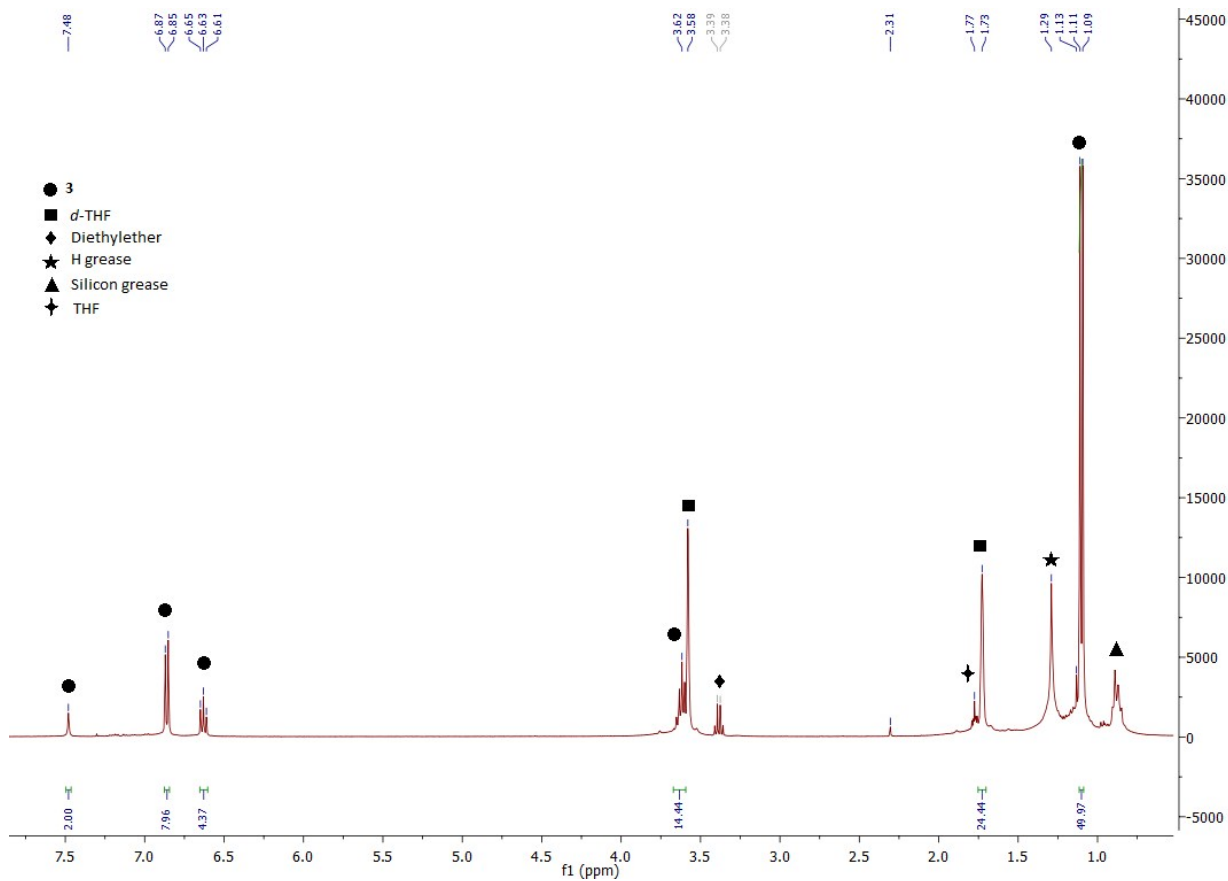


Figure S6. NMR spectrum of compound **3** in *d*-THF.

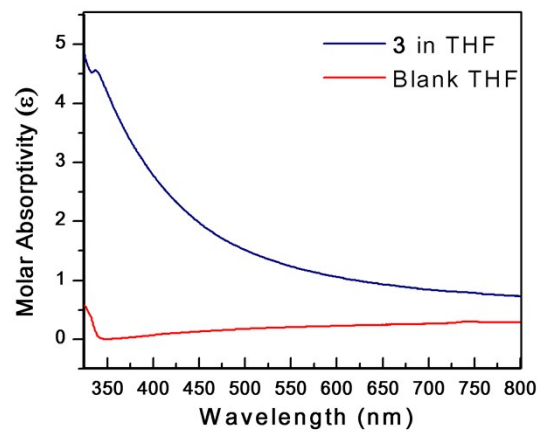


Figure S7. UV-vis spectrum of compound **3**.

References:

- (1) Schrock, R. R.; Sturgeooff, L. G.; Sharp, P. R. *Inorg. Chem.* **1983**, 22 (20), 2801.
- (2) Krahulic, K. E.; Enright, G. D.; Parvez, M.; Roesler, R. *J. Am. Chem. Soc.* **2005**, 127 (12), 4142.
- (3) Hohenberg, P.; Kohn, W. *Phys. Rev.* **1964**, 136 (3B), B864.
- (4) Calais, J.-L. *Int. J. Quantum Chem.* **1993**, 47 (1), 101.
- (5) Becke, A. D. *Phys. Rev. A* **1988**, 38 (6), 3098.
- (6) Becke, A. D. *J Chem Phys* **1993**, 98 (2).
- (7) Becke, A. D. *J. Chem. Phys.* **1993**, 98 (7), 5648.
- (8) Lee, C.; Yang, W.; Parr, R. G. *Phys. Rev. B* **1988**, 37 (2), 785.
- (9) Frisch, M. J.; Trucks, G. W.; Schlegel, H. B.; Scuseria, G. E.; Robb, M. A.; Cheeseman, J. R.; Scalmani, G.; Barone, V.; Mennucci, B.; Petersson, G. A.; Nakatsuji, H.; Caricato, M.; Li, X.; Hratchian, H. P.; Izmaylov, A. F.; Bloino, J.; Zheng, G.; Sonnenberg, J. L.; Hada, M.; Ehara, M.; Toyota, K.; Fukuda, R.; Hasegawa, J.; Ishida, M.; Nakajima, T.; Honda, Y.; Kitao, O.; Nakai, H.; Vreven, T.; Montgomery, Jr., J. A.; Peralta, J. E.; Ogliaro, F.; Bearpark, M.; Heyd, J. J.; Brothers, E.; Kudin, K. N.; Staroverov, V. N.; Kobayashi, R.; Normand, J.; Raghavachari, K.; Rendell, A.; Burant, J. C.; Iyengar, S. S.; Tomasi, J.; Cossi, M.; Rega, N.; Millam, N. J.; Klene, M.; Knox, J. E.; Cross, J. B.; Bakken, V.; Adamo, C.; Jaramillo, J.; Gomperts, R.; Stratmann, R. E.; Yazyev, O.; Austin, A. J.; Cammi, R.; Pomelli, C.; Ochterski, J. W.; Martin, R. L.; Morokuma, K.; Zakrzewski, V. G.; Voth, G. A.; Salvador, P.; Dannenberg, J. J.; Dapprich, S.; Daniels, A. D.; Farkas, O.; Foresman, J. B.; Ortiz, J. V.; Cioslowski, J.; Fox, D. J. *Gaussian 09, Revision A.1*; Gaussian, Inc.: Wallingford, CT, **2009**.